Food Chemistry 371 (2022) 131135

Contents lists available at ScienceDirect

Food Chemistry

journal homepage: www.elsevier.com/locate/foodchem

Impact of plasma reactive species on the structure and functionality of pea protein isolate

Fan Bu [a], Gaurav Nayak [b], Peter Bruggeman [b], George Annor [a], Baraem P Ismail [a,*]

[a] Food Science and Nutrition Department, University of Minnesota, 1334 Eckles Ave, Saint Paul, MN 55108, United States
[b] Department of Mechanical Engineering, University of Minnesota, 111 Church St SE, Minneapolis, MN 55455, United States

ARTICLE INFO

Keyword:
Cold atmospheric plasma
Reactive oxygen and nitrogen species
Pea protein isolate
Pea protein structure and functionality

ABSTRACT

The impact of plasma-produced reactive oxygen and nitrogen species, in particular O_3, N_xO_y, H_2O_2 and OH, on the structure and functionality of pea protein isolate (PPI) was evaluated. Reactive species were produced through a combination of controlled measurements and plasma treatments. Pronounced structural and functional effects were observed upon treatment with reactive species at pH 2. All reactive species induced protein denaturation and the formation of disulfide-linked soluble aggregates. A significant increase in surface hydrophobicity and β-sheet content was only induced by treatment with O_3 and OH. These specific changes resulted in significant enhancement in gelation and emulsification. While H_2O_2 enhanced PPI color by increasing whiteness, it had the least impact on protein structure and functionality. Results of this work can be used to optimize cold atmospheric plasma treatment of PPI to induce specific structural changes and a directed enhancement in functionality.

1. Introduction

The global plant protein ingredient market is projected to accumulate $15.65 billion in revenue by 2024 (Market Research Future, 2021). The steep increase in the plant protein market is largely attributed to environment and animal welfare concerns, as well as awareness of the health benefits of plant proteins (Ismail, Senaratne-Lenagala, Stube, & Brackenridge, 2020). Soy protein, a nutritious and functional protein, remains the dominant protein in the plant protein market. However, soy is one of the "Big Eight" allergens and is mostly a genetically modified (GMO) crop. Therefore, consumers are seeking alternatives to soy protein, and the food industry accordingly is searching for effective replacement, one being pea protein (Ismail et al., 2020).

Pea protein is rapidly replacing soy protein in the market due to readily available non-GMO sources (yellow field peas), low cost of production, nutritional benefits, and low occurrence of allergenicity (Barac et al., 2010). However, the functional properties of pea protein ingredients (e.g. solubility, gelation and emulsification) are inferior to those of soy protein counterparts. Inferior functionality is largely attributed to the intrinsic protein profile and structure. Additionally, pea protein lags behind soy protein in the development of isolation and processing technologies. To better compete with soy protein, the functional properties, such as gelation and emulsification, of pea protein must be enhanced.

To enhance the functionality of pea protein ingredients, research has focused on modifying the inherent protein structure. Protein modification included enzymatic hydrolysis (Barać et al., 2011), Maillard-induced glycation (Kutzli et al., 2020), and physical modifications (Mirmoghtadaie, Shojaee Aliabadi, & Hosseini, 2016). Protein enzymatic hydrolysis is widely used in industry to produce hydrolysates with

Abbreviations: ATR-FTIR, attenuated total reflectance Fourier transform infrared spectroscopy; APPJ, atmospheric pressure plasma jet; CAP, cold atmospheric plasma; cPPI, commercial pea protein isolate; DBD, dielectric barrier discharge; DH, degree of hydrolysis; DSC, differential scanning calorimetry; EC, emulsification capacity; mPPI, plasma species modified pea protein isolate; mPPI- N_xO_y/O_3 pH 2, N_xO_y/O_3 mixture modified pea protein isolate at pH 2; mPPI- N_xO_y/O_3 pH 7, N_xO_y/O_3 mixture modified pea protein isolate at pH 7; mPPI- O_3 pH2, O_3 modified pea protein isolate at pH 2; mPPI- O_3 pH 7, O_3 modified pea protein isolate at pH 7; mPPI- H_2O_2 pH 2, H_2O_2 modified pea protein isolate at pH 2; mPPI- H_2O_2 pH 7, H_2O_2 modified pea protein isolate at pH 7; mPPI- OH pH 2, OH radicals modified pea protein isolate at pH 2; mPPI- OH pH 7, OH radicals modified pea protein isolate at pH 7; PPI, pea protein isolate pea protein isolate; PPI control- pH7, untreated PPI control at pH 7; PPI control- pH2, untreated PPI control at pH 2; RNS, reactive nitrogen species; ROS, reactive oxygen species; SDS-PAGE, sodium dodecyl sulphate-polyacrylamide gel electrophoresis; SE-HPLC, size-exclusion high-performance liquid chromatography.

* Corresponding author.
E-mail address: bismailm@umn.edu (B.P. Ismail).

https://doi.org/10.1016/j.foodchem.2021.131135
Received 4 April 2021; Received in revised form 30 August 2021; Accepted 12 September 2021
Available online 15 September 2021

enhanced functionality and nutritional value (Ge et al., 2020). Pea protein hydrolysates demonstrated better solubility, and enhanced emulsifying and foaming properties compared to pea protein isolates (Barac et al., 2012; Barać et al., 2011). However, the degree of hydrolysis (DH) is strongly correlated to bitterness, compromising the sensory quality of the ingredient (Arteaga, Guardia, Muranyi, Eisner, & Schweiggert-Weisz, 2020). Mallard-induced glycation has also been shown to improve the solubility of pea protein (Kutzli et al., 2020). However, research in this area is only emerging and further investigations are required to make the process industrially feasible with limited adverse effects, such as the production of advanced glycation products (Lin et al., 2020). Traditional physical modifications of pea protein, such as heating (Chao & Aluko, 2018) and extrusion (Osen, Toelstede, Wild, Eisner, & Schweiggert-Weisz, 2014), have been explored as well. Heat is a key component of traditional physical modification methods that can induce partial denaturation of proteins and the formation of high molecular weight soluble aggregates (Mirmoghtadaie et al., 2016). Traditional, heat-based physical modifications contribute to modestly enhanced solubility, oil holding capacity, emulsification, foaming, and texturization properties of pea protein (Chao & Aluko, 2018; Chao, Jung, & Aluko, 2018; Osen et al., 2014). The biggest concern of high temperature processing includes the reduction of nutritional quality attributed to a significant loss of lysine due to the Maillard reaction, and a decrease in digestibility due to excessive polymerization (Björck & Asp, 1983). Additionally, traditional physical modifications require high energy input, which increase the cost of production.

Cold atmospheric plasma (CAP), an ionized gas near room temperature, enables the production of reactive oxygen and nitrogen species at ambient temperatures and is being explored as a novel physical protein modification method. Key advantages of the approach include its operation at ambient temperature and the potential for high energy efficiency. Considerable research explored the utilization of CAP for waste management (Harris, Phan, & Zhang, 2018), water disinfection (Prakash et al., 2017), microbial inactivation (Moldgy, Nayak, Aboubakr, Goyal, & Bruggeman, 2020), wound healing (Boekema et al., 2015), and enzyme inactivation (Pankaj, Misra, & Cullen, 2013). Cold plasma is produced by subjecting gases, such as air, oxygen, and argon, to a high voltage, typically applied across two metal electrodes. The resulting electric field enables ionization and acceleration of energetic electrons that lead to dissociation of molecules resulting in a cocktail of highly reactive oxygen species (ROS) (O, O_3, OH, H_2O_2) and reactive nitrogen species (RNS), NO_2 and N_2O_5 (Gorbanev, Privat-Maldonado, & Bogaerts, 2018). Different gases and plasma generating approaches result in various profiles of reactive species, which may induce different chemical reactions, such as oxidation, polymerization, and bond cleavages (Tolouie, Mohammadifar, Ghomi, & Hashemi, 2018). For example, dielectric barrier discharge (DBD), i.e. a plasma generated between two metal electrodes covered by a dielectric material, is one of the most effective plasma configurations enabling the production of O_3 using air or O_2 (Bahrami et al., 2016). Hydroxyl radicals (OH) and hydrogen peroxide (H_2O_2), on the other hand, are produced when water vapor is present in the feed gas (Bruggeman & Schram, 2010).

The utilization of CAP as a physical modification of food proteins has also garnered interest. Recently, several studies reported the impact of CAP on plant and animal proteins (Ji et al., 2018; Sharifian, Soltanizadeh, & Abbaszadeh, 2019), with few reports on the impact of CAP on pea proteins (Bußler, Steins, Ehlbeck, & Schlüter, 2015; Mahdavian Mehr & Koocheki, 2020). Bußler et al. (2015) reported an increase in solubility and water binding capacity of pea protein after DBD treatment. Improvement in emulsion properties and solubility of pea protein after a short-time DBD treatment was also reported by Mahdavian Mehr and Koocheki (2020). While the reported findings are promising, it remains unclear how plasma-induced structural changes impacted functionality. Additionally, the link between different plasma species and the observed structural changes, and consequent functional enhancement, was not demonstrated in similar studies on impact of CAP on protein functionality. Therefore, the objective of this study was to evaluate the impact of plasma reactive species (N_xO_y, O_3, H_2O_2, OH) on the structure and functionality of pea protein isolate. This study will demonstrate the impact of different plasma-produced reactive species on protein structural changes, and will provide basic information needed for identifying optimal CAP treatment (plasma generation approach and feed gas) to produce functionally enhanced pea protein ingredients.

2. Materials and methods

2.1. Materials

Yellow field pea flour was kindly provided by AGT Foods (Regina, SK, Canada). Defatted soy flour (7B, 53% protein) was kindly provided by Archer Daniels Midland (ADM) (Decatur, IL, USA). Commercial pea protein isolate (cPPI, 81.2% protein, 3.86% ash) PURIS™, was kindly provided by Puris Foods (Minneapolis, MN, USA). Samples were stored at −20 °C before the usage. Criterion™ TGX™ 4–20% precast gels, Laemmli sample buffer, 10X Tris/Glycine/sodium dodecyl sulfate (SDS) running buffer, Imperial™ Protein Stain, and Precision Plus molecular weight marker were purchased from Bio-Rad Laboratories, Inc. (Hercules, CA, USA). Superdex™ 200 Increase 10/300 GL Prepacked Tricorn™ Column, gel filtration LMW calibration kit, and gel filtration HMW calibration kit were purchased from Cytiva (Marlborough, MA, USA). SnakeSkin™ dialysis tubing with 3.5 kDa molecular weight cut off (MWCO) and Sudan Red 7B were purchased from Thermo Fisher Scientific™ (Waltham, MA, USA). Aluminum crucibles (40 μL, with pin) for DSC were purchased from Mettler-Toledo (Columbus, OH, USA). Folded capillary cuvettes for zeta potential were purchased from Malvern (Malvern, UK). Costar® solid opaque black 96-well plates and 8-anilino-1-napthalenesulfonic acid ammonium salt (ANS) were purchased from Sigma-Aldrich (St. Louis, MO, USA). Pure corn oil (Mazola) was purchased from a grocery store. All other analytical grade reagents were purchased from Thermo Fisher Scientific or Sigma-Aldrich.

2.2. Preparation of pea protein isolate (PPI)

Pea protein isolate (PPI) was produced following a pH extraction method (alkaline solubilization with isoelectric precipitation extraction). Pea flour was fully dispersed in a tenfold volume of double distilled water (DDW) and adjusted to pH 7.5 with 2 N NaOH. Protein slurries were stirred for 1 h at room temperature, then centrifuged at 5000×*g* for 30 min to precipitate insoluble materials. The pellet was re-suspended in a tenfold volume of DDW and adjusted to pH 7.5 for another 1-hour solubilization, followed by 30-minutes centrifugation at 5000×*g*. Supernatant from both solubilizations were combined and adjusted to the isoelectric point (pH 4.5), followed by 10-minutes centrifugation at 5000×*g* to precipitate the protein. The protein pellet was then re-suspended in DDW (1:4 w/v), neutralized, dialyzed, and lyophilized. The solid yield of PPI (17.2%) and total protein yield (64.7%) were determined by mass balance. The protein content of PPI (89.8%) was determined by the Dumas method (AOAC 990.03), using a LECO® FP828 nitrogen analyzer (LECO, St. Joseph, MI, USA), with a conversion factor of 6.25.

2.3. Plasma species treatment

2.3.1. Ozone (O_3) and reactive nitrogen species (RNS) treatment

The flow-through plasma reactor used in this work (Fig. 1) was configured based on the work by Nayak, Aboubakr, Goyal, and Bruggeman (2018). Briefly, the reactor consisted of an electrode arrangement embedded in a homemade electrode holder made of polytetrafluoroethylene (PTFE). The holder allows for applying a gas flow through the electrode where it is treated by the plasma. The electrode is a two-dimensional array of 105 integrated coaxial micro-holes (600 μm in

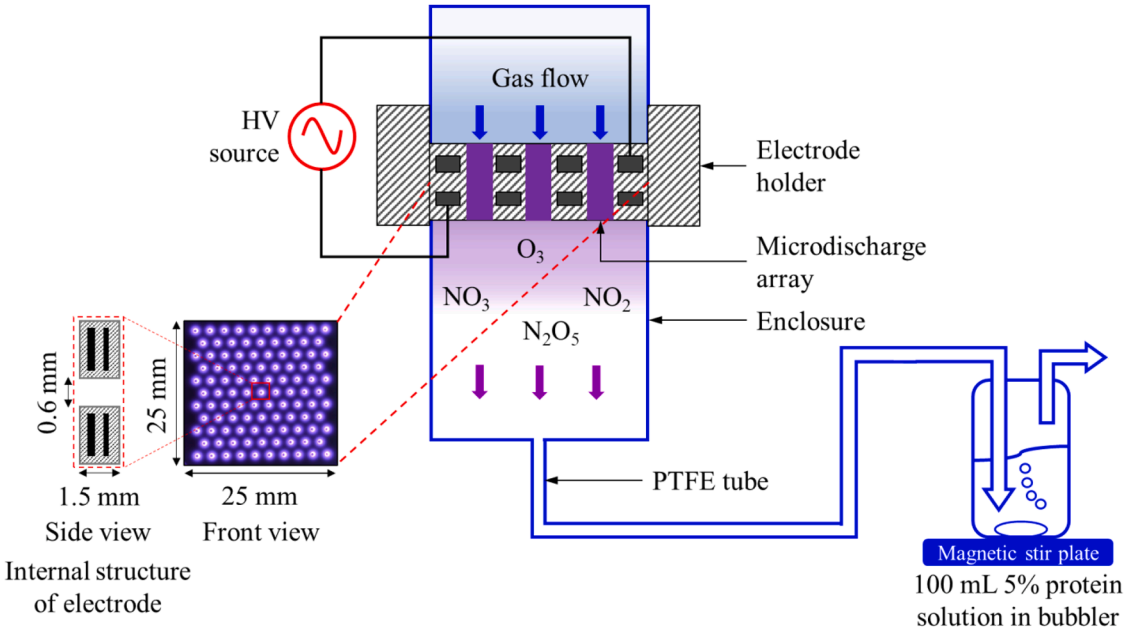

Fig. 1. A schematic of the 2D-DBD apparatus used for generating N_xO_y/O_3 and O_3 plasma reactive species using air and Ar + 20% O_2, respectively, at a total gas flow rate of 5 slm.

diameter) punched through two internal and parallel ultra-thin metal (gold and nickel) plates covered and separated by alumina as the dielectric material. One of the metal plates was powered while the other was grounded. The discharge was ignited in these micro-holes by applying a high voltage sinusoidal signal at 20 kHz generated by an AC power source (PVM500, Information Unlimited), and is referred to as the two-dimensional dielectric barrier discharge or 2D-DBD. The power was measured using the Lissajous method as previously described (Nayak, Du, Brandenburg, & Bruggeman, 2017) by measuring the high voltage across the electrode using a high-voltage probe (Tektronix P6015A), and the charge across a 20 nF capacitor on the grounded side using a passive voltage probe (Tektronix TPP0200).

The discharge was operated at atmospheric pressure in dry air (Laboratory Grade) as well as in argon (Ar) with 20% admixture of O_2 (Ultra-Pure-Carrier Grade 99.9993%) at a constant total gas flow rate of 5 standard liters per minute. The plasma power was kept constant at 14.5 ± 0.1 W in air and at 10.3 ± 1.1 W in Ar/O_2. The air plasma was used to generate reactive oxygen and nitrogen species (RONS), while the Ar/O_2 plasma dominantly produced O_3 as the long-lived species. The ozone densities in air and Ar/O_2 plasmas were $(1.6 \pm 0.1) \times 10^{22}$ m^{-3} and $(1.4 \pm 0.2) \times 10^{22}$ m^{-3}, respectively, as measured with the UV absorption spectroscopy at 253.4 nm (Nayak, Sousa, & Bruggeman, 2017).

For protein treatment, the effluent of the 2D-DBD confined within a polycarbonate tube was sent through a 100 mL protein solution (5% w/v protein in DDW) in a bubbler (PYREX® 500 mL Gas Washing Bottle with Coarse Fritted Cylinder) for treatment time of 30 min. The gas residence time in the effluent of the plasma till it reaches the protein solution is ~ 12 s. As such, for Ar/O_2 plasma, O_3 is the dominant reactive species reaching the protein solution. For air plasma, owing to such large timescales, O_3 could react with RNS to form NO_2 and N_2O_5. With a larger Henry's law solubility constant compared to NO and NO_2, N_2O_5 will more readily dissolve in the protein solution to produce subsequent secondary reactive chemistry in the liquid-phase (Moldgy et al., 2020).

2.3.2. H_2O_2 treatment

To investigate the effect of hydrogen peroxide (H_2O_2) on protein, 100 mL of 3 mM H_2O_2 was added to 100 mL of protein solution (5% w/v protein in DDW). The final concentration of H_2O_2 was1.5 mM.

2.3.3. OH radical treatment

To determine the effect of hydroxyl (OH) radical on the protein structure and functionality, Fenton's reaction (Pignatello, Oliveros, & MacKay, 2006) was used to generate OH radicals in the bulk of the protein solution. For this, 50 mL of 6 mM H_2O_2 was added to 100 mL of protein solution (5% w/v protein in DDW), followed by the addition of 50 mL of 6 mM ferrous sulfate ($Fe(II)SO_4$) solution. This results into a final concentration of equimolar concentrations of H_2O_2 and Fe(II) ions (1.5 mM) generating OH radicals in the bulk of the solution.

2.3.4. Handling of the protein solutions

PPI solutions (5% w/v protein in DDW) were prepared, in triplicate, at pH 2 or pH 7, for all four plasma species treatments, to evaluate the impact of plasma species on structural and functional changes. Since a decrease in pH, close to the isoelectric point (pI, pH 4.5) of pea protein after plasma treatment, was observed in our preliminary studies and other published work (Ekezie, Cheng, & Sun, 2019), protein solutions were adjusted to pH 2, where protein remained charged and soluble, to avoid protein precipitation during the treatment. The two pH treatments allowed for the observation of different chemical reactions and intensities induced by the different plasma species. Solutions of modified pea protein isolates (mPPIs) at both pHs were adjusted to pH 7 immediately after treatment. An additional dialysis step was applied to mPPIs at pH 2 to achieve the same protein and ash content as that of mPPIs treated at pH 7. After pH adjustment, mPPIs were lyophilized and stored at 4 °C. In addition, non-dialyzed mPPIs treated at pH 2 were also collected to evaluate the effect of higher salt content (as a result of pH adjustments) on their structure and functionality. Protein content of lyophilized mPPIs was determined following the Dumas method, and ash content was determined by the AOAC dry ashing method (AOAC 942.05).

2.4. Color measurement

The color of PPI, cPPI and plasma modified samples was assessed, in triplicate, using a Chroma Meter CR-221 (Minolta Camera Co., Osaka, Japan). Before analysis of the samples, the Chroma Meter was calibrated with a white CR-221 calibration plate (Minolta). The color of the samples was recorded using the CIE (International Commission on

Illumination) 1976 L* a * b * color space system, where L* indicates lightness, ranging from 0 (black) to 100 (white); positive a* values represent red; negative a* values represent green; positive b* values represent yellow, while negative b* values represent blue. To assess the effect of plasma species treatment on color, total color difference (ΔE) between modified and non-modified PPI was calculated.

2.5. Protein profiling by gel electrophoresis

Protein profiling of PPI, cPPI and plasma modified samples (mPPIs) was performed using sodium dodecyl sulfate polyacrylamide gel electrophoresis (SDS-PAGE), as described by Boyle, Hansen, Hinnenkamp, and Ismail (2018). Briefly, samples (5 μL; containing ~ 50 μg protein) and Precision Plus™ MW standard (10 μL) were loaded onto a Criterion™ TGX™ 4–20% precast Tris-HCl gradient gel. The gel was electrophoresed, stained/destained, and imaged as outlined by Boyle et al. (2018).

2.6. Molecular weight distribution by size-exclusion – high-performance liquid chromatography (SE-HPLC)

PPI, cPPI and mPPIs were subjected to size-exclusion HPLC (SE-HPLC) using a Shimadzu HPLC system (Shimadzu Scientific Instruments, Colombia, MD, USA) equipped with SIL-10AF auto injector, LC-20AT pump system, CTO-20A column oven, SPD-M20A photo diode array detector, and a CBM-20A communication module. A Superdex 200 Increase 10/300 GL Prepacked Tricorn™ Column was used to separate proteins based on molecular weight. The analysis was performed at room temperature following the method of Brückner-Gühmann, Heiden-Hecht, Sözer, and Drusch (2018), with modifications. Samples (1% protein, w/v), in triplicate, were solubilized in pH 7 phosphate buffer (0.05 M sodium phosphate with 0.1 M sodium chloride) at room temperature for 2 h, then passed through a 0.45 μm filter, automatically injected (100 μL) and separated isocratically using pH 7 phosphate buffer mobile phase at a flow rate of 0.5 mL per minute for a total run time of 80 min. Detection and analysis were performed at 280 nm. Molecular weights were calculated by running gel filtration calibration standards (HMW and LMW kits). Relative peak areas—the ratio of the area of a single peak to total peak area for a sample—were used to monitor differences in molecular weight distribution among the samples. Peak identities were assigned based on reported molecular weights (Barac et al., 2010; Gatehouse, Lycett, Croy, & Boulter, 1982; Tzitzikas, Vincken, De Groot, Gruppen, & Visser, 2006).

2.7. Differential scanning calorimetry (DSC)

Protein denaturation temperature and enthalpy of the different samples were determined using a DSC instrument (DSC 1 STARe System, Mettler Toledo, Columbus, OH, USA), according to the method outlined by Boyle et al. (2018). Samples, in triplicate, were solubilized in DDW (20% protein, w/v) and stirred overnight at room temperature. An aliquot (20 μL, delivering approximately 4 μg protein) was transferred to an aluminum pan and hermetically sealed. An empty sealed pan was run simultaneously as reference. The pans were held at 25 °C for 5 min, then heated from 25 °C to 110 °C at an increment rate of 5 °C/min. Thermograms were manually integrated to obtain the peak denaturation temperature and enthalpy of denaturation for each protein using Mettler Toledo's STARe Software version 11.00.

2.8. Attenuated total reflectance Fourier transform infrared spectroscopy (ATR-FTIR)

ATR-FTIR spectra of modified and non-modified protein isolates were recorded using Fourier transform infrared spectrometer (Thermofisher Nicolett iS50 FTIR). Protein lyophilized powders were placed on diamond ATR and scanned from 400 to 4000 cm^{-1} by DLaTGS detector. ATR spectra were converted to transmission spectra using OMNIC® software. Second derivative of Amide I band (1600 cm^{-1} –1700 cm^{-1}) were obtained by PeakFit v. 4.12 to identify alpha-helix, beta-sheet, beta-turn, and random coil.

2.9. Measurement of protein surface properties

Surface hydrophobicity was determined fluorometrically using an 8-anilino-1-napthalenesulfonic acid ammonium salt (ANS) probe, based on the method outlined by Boyle et al. (2018), with modifications in fluorescence gain (40) and the use of black 96-well plate. Zeta potential was measured using a dynamic light scattering instrument (Malvern Nano Z-S Zetasizer). Protein solutions (10 mL of 0.1% protein in DDW, w/v), in triplicate, were adjusted to pH 7, and stirred for 2 h. An aliquot (1 mL) of each solution was dispensed into a folded capillary cell and inserted into the Zetasizer. After a 30 s equilibration period, electrophoretic mobility was measured by two sub-rep readings taken every 10 s for each replicate. Zeta potential was determined by Malvern's Zetasizer software (version 7.13) using the Smoluchowski model.

2.10. Protein solubility

Protein solubility at pH 7 was determined following the method described by Boyle et al. (2018), with modifications in sample size (5 mL), protein concentration, and duration of solubilization (2 h). Protein solutions (5 mL) were prepared, in triplicate, at 5% protein (w/v in DDW) and adjusted to pH 7 using 2 N NaOH and an Orion™ ROSS Ultra™ pH Electrode (Thermo Scientific). Samples were assessed at room temperature and post thermal treatment (80 °C for 30 min). Solubility was expressed as the percentage of soluble protein (present in the supernatant post centrifugation) compared to the total protein content determined following the Dumas method.

2.11. Gel strength

Strength of heat-induced gels was determined following the method described by Boyle et al. (2018), with modifications. Protein solutions (5 mL) were prepared, in triplicate, at 15% and 20% protein (w/v, in DDW), adjusted to pH 7, and stirred for 2 h. Aliquots (1 mL) were dispensed into lightly oiled microcentrifuge tubes using a positive displacement pipette. Samples were heated in a water bath at 95 °C (±2 °C) for 20 min. After cooling to room temperature, gels were removed from the microcentrifuge tubes and gel strength was measured by a TA-TX Plus Texture Analyzer (Stable Micro Systems LTD, Surrey, UK) using a 100 mm diameter probe, 5 mm/s test speed, and a target distance of 0.5 mm from the plate. The maximum force measured in Newton was the rupture force of the gel.

2.12. Emulsification capacity

Emulsification capacity (EC) was determined following the methods outlined by Boyle et al. (2018) with modifications in the sample solubilization protocol and the oil titration speed. Protein samples, in triplicate, were solubilized in DDW (20 mL, at 2% protein concentration, w/v), adjusted to pH 7, and stirred for 2 h. Corn oil dyed with Sudan Red 7B was titrated into an aliquot of each protein solution (5 mL) at a steady flow rate of 2 mL per min for the first 3 min and then increased to 6 mL per min for the remainder of the titration, while blending using a homogenizer (IKA® RW 20 Digital, IKA Works Inc., Wilmington, NC, US) with a 4 blade, 50 mm diameter shaft (IKA® R 1342) rotating at 860–870 rpm. Samples were homogenized while titrating with oil until a phase inversion was observed. Emulsification capacity was expressed as g of oil emulsified by one g of protein.

2.13. Statistical analysis

Analysis of variance (ANOVA) was determined using SigmaPlot software version 14.0 for windows (Systat Software, San Jose, CA). Tukey-Kramer multiple means comparison test was used to determine significant differences ($P \leq 0.05$) between the means ($n = 3$) of at least three different samples. A student's unpaired *t*-test was used to test for significant differences ($P \leq 0.05$) between the means ($n = 3$) of two different samples.

3. Results and discussion

3.1. Protein and ash content of treated and untreated pea protein isolates

The protein and ash contents (total amount of minerals) of the control PPI and mPPIs treated at pH 7 were in the range of 89.6–91.2% and 3.8–4.5%, respectively. The protein and ash contents of the control PPI and mPPIs treated at pH 2 were in the range of 80.0–84.5% and 10.1–15.1%, respectively. The decrease in protein content and increase in ash content in the mPPIs treated at pH 2 were attributed to the formation of NaCl after several pH adjustments, as well as the formation of salts by dissolving long-lived plasma species into the protein solutions. An additional dialysis step was performed for the mPPIs treated at pH 2 to obtain similar protein (89.8–92.2%) and ash (3.8–4.5%) contents as those of mPPIs treated at pH 7.

3.2. Effect of plasma species on the color of the isolates

An increase in the total color difference (ΔE) of PPI was observed after plasma species (N_xO_y/O_3, O_3, H_2O_2, and OH) treatment at pH 2 (Table S1). Similarly, Bußler et al. (2015) reported an increase in ΔE of pea protein powder after DBD (air) treatment, which was comprised of N_xO_y and O_3 species. A decrease in lightness (L*) and an increase in green color were observed after RNS/O_3 treatment. Also, O_3 treatment alone significantly decreased the lightness compared to PPI controls. However, H_2O_2 resulted in a significant increase in L* compared to PPI controls. This observation is reasonable given the fact that food-grade H_2O_2 is usually used as a bleaching agent during food processing (Farr, Smith, & Steichen, 2000). mPPI treated with OH radicals at pH 2 (mPPI- OH pH2) demonstrated the largest ΔE, which was mostly attributed to the reduction in yellow color (Table S1). Segat, Misra, Cullen, and Innocente (2015) reported an increase in the yellow color of whey protein solution after DBD (air) treatment, under a similar setup and gas as in this study. However, none of the reactive species in this study significantly increased the yellow color of PPI, unlike the observation of Segat et al. (2015), who attributed the increase in yellow color to O_3 species. Since protein samples were dissolved in phosphate buffer during the plasma treatment in the study by Segat et al. (2015), it is possible that phosphorylation of protein happened during the DBD treatment, resulting in the increase in yellow color (Kaewruang, Benjakul, Prodpran, Encarnacion, & Nalinanon, 2014). In this study, plasma species generally did not impart major changes in color that may impact negatively the physical quality of the protein powders.

3.3. Effect of plasma species on protein profile and changes in molecular weight

Plasma treatments at both pH 7 and pH 2 resulted in protein polymerization compared to the control PPI, as indicated by the smearing in the upper molecular weight region of the gel (Fig. 2**a & b**). Under reducing conditions, the smearing was no longer evident, indicating that the polymerization was via disulfide linkages. As oxidants, the plasma reactive species promoted disulfide interchange. Mahdavian Mehr and Koocheki (2020) and Nyaisaba et al. (2019) found protein polymerization after DBD (air) treatment of pea protein and squid protein, respectively. Again, plasma generated by remote DBD with air is a

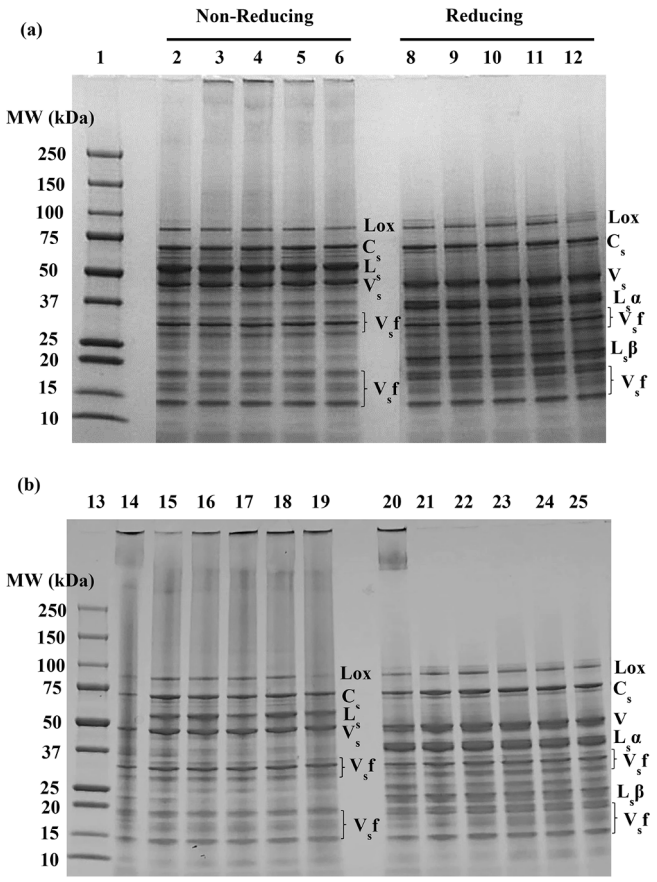

Fig. 2. SDS-PAGE gel visualization of the protein profiles of the PPI samples treated at (a) pH 7 and (b) pH 2 and a reference sample (cPPI) under nonreducing (lane 2–6 and lane15-20) and reducing (lane 8–12 and lane 21–25) conditions. Lane 1,14: Molecular weight (MW) marker; Lane 2, 8: PPI Control-pH 7; Lane 14,20: cPPI reference; Lane 3, 9: mPPI- N_xO_y/O_3 pH7; Lane 4, 10: mPPI- O_3 pH7; Lane 5, 11: mPPI- H_2O_2 pH7; Lane 6, 12: mPPI- OH pH7; Lane 15, 21: cPPI; Lane 16, 22: PPI Control-pH2; Lane 17, 23: mPPI- N_xO_y/O_3 pH2; Lane 18, 24: mPPI- O_3 pH2; Lane 19, 25: mPPI- H_2O_2 pH2; Lane 20, 26: mPPI-OH pH2. Lox: lipoxygenase; C_s: subunits of convicilin; V_s: subunits of vicilin; $L_s\alpha$: acidic peptides cleaved from legumin subunits; $L_s\beta$: basic peptide cleavage from legumin subunit; V_sf: fractions of vicilin subunits result from post-translational cleavages.

mixture of O_3 and N_xO_y, on timescales corresponding to protein treatment in this study (~12 s). O_3 in this study induced protein polymerization (Fig. 2**a & b**). Therefore, the protein polymerization reported by Mahdavian Mehr and Koocheki (2020) and Nyaisaba et al. (2019) could be attributed to O_3. Since N_xO_y/O_3 mixture induced similar protein polymerization as well (Fig. 2**a, lane 3,** Fig. 2**b, lane 16**), a further study with RNS alone may elucidate its individual effect on protein polymerization.

Comparing the smearing intensity in lanes 15–19 (Fig. 2**b**) to lanes 2–6 (Fig. 2**a**), it is apparent that plasma species treatment at pH 2 resulted in more polymerization than treatment at pH 7. To a lesser degree, high molecular weight polymers were also observed in pH 2 PPI control, while none were evident for pH 7 PPI control. This observation, indicated that, independent of plasma species treatment, extreme acidic pH caused protein unfolding due to like charges and disruption of ionic bonding within the protein. Unfolded protein will have higher tendency to polymerize due to the exposure of hydrophobic groups as well as sulfhydryl groups. However, the degree of polymerization at pH 2, as evident by darker smearing, was intensified upon plasma species treatment (Fig. 2**b, lanes 16–19**). The formation of high molecular weight polymers that may remain soluble (i.e. soluble aggregates) can enhance

functional properties, namely gelation and emulsification (Mahdavian Mehr & Koocheki, 2020).

Under non-reducing conditions, highly polymerized proteins were apparent in cPPI, analyzed as a reference protein **(**Fig. 2**b, lane 14)**, as noted by the smearing and presence of dark bands at the top of the gel. Under reducing conditions, the smearing was less apparent, yet distinct high intensity bands remained in the upper part of the gel, indicating that some of the polymers in cPPI are formed by covalent linkages other than the covalent disulfide interactions **(**Fig. 2**b, lane 20)**. Such high level of polymerization in this case may be detrimental to the functional properties.

The molecular weight distribution of soluble aggregates, legumin, vicilin, and convicilin proteins were further characterized using SE-HPLC. The relative abundance of soluble aggregates, functional proteins (legumin, vicilin and convicilin), and low molecular weight proteins is shown in Fig. 3 and Table 1. Neither non-covalent interactions nor disulfide linkages among the protein subunits were disrupted during the analysis due to the absence of SDS and a reducing agent. Therefore, additional information on protein profile and molecular distribution as influenced by plasma reactive species was obtained.

The molecular weight of soluble aggregates was about 1200 kDa, while that of hexameric legumin, trimeric convicilin, and trimeric vicilin **(**Table 1**)** fell within the expected ranges (Barac et al., 2010; Gatehouse et al., 1982; Tzitzikas et al., 2006). Insoluble aggregates did not pass through the 0.45 μm filter and thus were not observed. In cPPI, the abundance of functional proteins was low **(**Fig. 3**)**, with only a small percentage of vicilin present **(**Table 1**)** relative to other smaller molecular weight polypeptides. The low relative abundance of functional proteins and soluble aggregates in cPPI confirmed that most of the functional proteins formed insoluble aggregates, thus were filtered out prior to the analysis.

In comparison to pH 7 control, mPPI treated with OH radicals at pH 7 (mPPI-OH pH7) had significantly lower relative abundance of legumin, convicilin and vicilin, accompanied by a significantly higher abundance

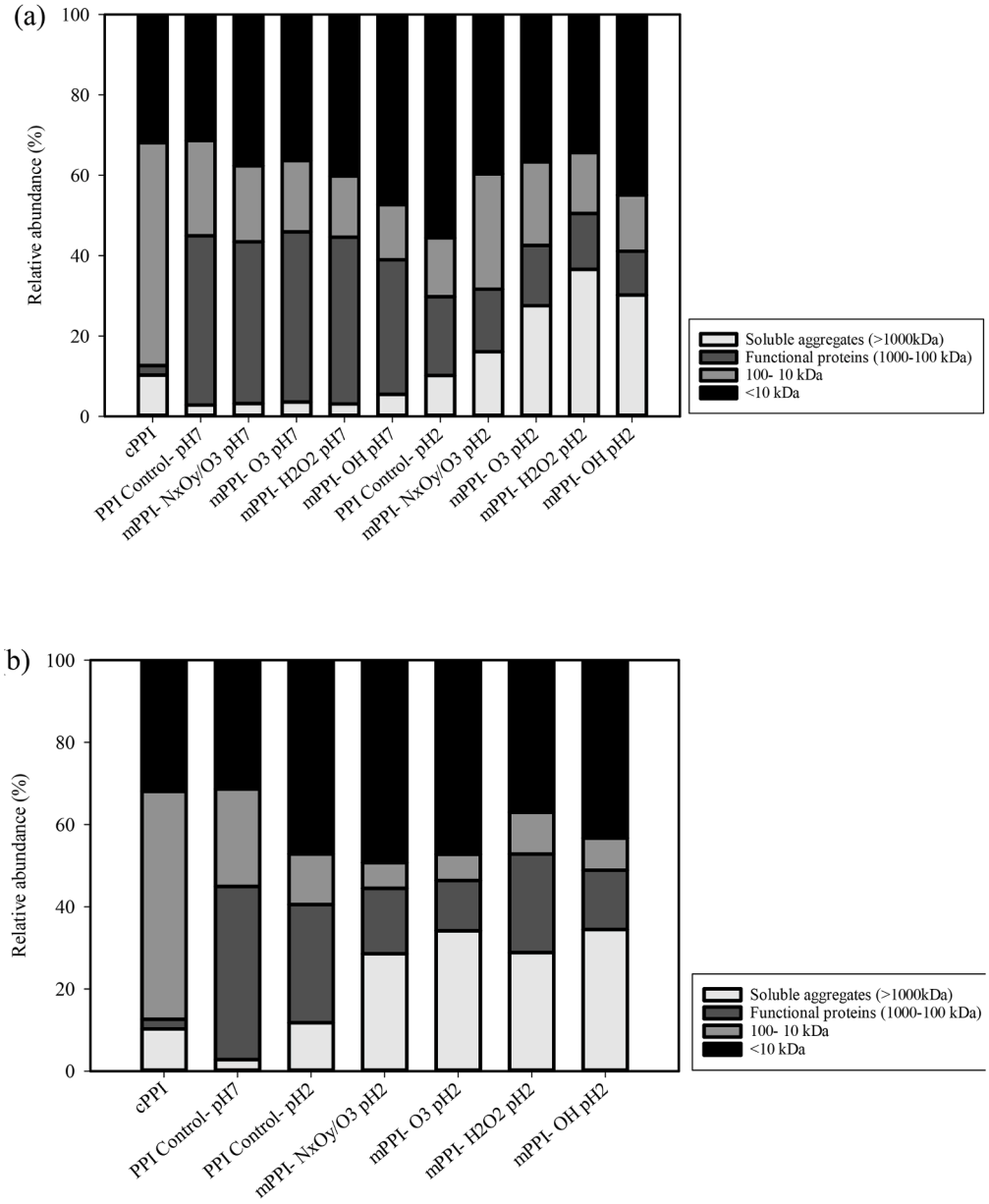

Fig. 3. Percent relative abundance of different protein fractions in commercial pea protein reference, non-modified pea protein controls, modified pea protein isolates at pH7 and pH 2 without dialysis (a), and modified pea protein isolates at pH 2 with dialysis (b). Samples were dissolved in pH 7 phosphate buffer and analyzed by size-exclusion high-performance chromatography (SE-HPLC). Bars distribution represents means of n = 3.

Table 1
Molecular weight and relative abundance of soluble aggregates, legumin, convicilin, and vicilin present in commercial pea protein reference, non-modified pea protein controls, and plasma modified pea protein isolates at pH 2 (with dialysis), as analyzed by size-exclusion high-performance liquid chromatography (SE-HPLC).

Protein Fractions[1]	Molecular weight (kDa)	Relative Abundance (%)[2]						
		cPPI	PPI Control-pH7	PPI Control-pH2	mPPI- N_xO_y/O_3 pH2	mPPI- O_3 pH2	mPPI- H_2O_2 pH2	mPPI- OH pH2
Soluble aggregates (association of legumin, vicilin and other protein fractions)	~1200	10.27[4b]	2.82[b]	11.80[b]	28.57[a]	34.16[a]	28.83[a]	34.43[a]
Legumin	~450	*[3]	22.01[a]	10.11[b]	5.12[c]	4.43[c]	10.14[b]	4.86[c]
Convicilin	~ 250	*	8.52[ab]	8.97[a]	5.21 [cd]	3.84[de]	6.94[bc]	4.70[d]
Vicilin	~160	2.36[e]	11.59[a]	9.64[b]	5.62 [cd]	3.99[d]	6.94[c]	4.92[d]

[1]Samples were dissolved in pH 7 phosphate buffer and analyzed by high-performance size exclusion chromatography (SE-HPLC);
[2]Relative abundance (%) is the area of a specific peak divided by the total peak area for that sample;
[3]An asterisk (*) represents no peak was apparent in this molecular weight range;
[4]Means (n = 3) in each row with different lowercase letters indicate significant differences according to the Tukey-Kramer multiple means comparison test ($P < 0.05$).

of soluble aggregates (Table S2). Treatment with O_3, N_xO_y/O_3 mixture, and H_2O_2 at pH 7 resulted in a significant decrease in the relative abundance of convicilin and vicilin, but not legumin, and a slight increase in soluble aggregates. The salt content in the non-dialyzed samples treated at pH 2, including the pH 2 control, contributed to a marked increase in soluble aggregates accompanied by a major decrease in legumin and vicilin (Table S2). The presence of salt is known to enhance protein association. The impact of plasma species treatment was masked by the presence of salt. Dialysis to remove excess salt was, therefore, necessary to observe the actual impact of plasma species at acidic pH on the protein molecular association and distribution.

After dialysis, results showed that all plasma species, N_xO_y/O_3 mixture, O_3, H_2O_2, and OH radicals at pH 2 resulted in a significant increase in soluble aggregates, coupled with a significant decrease in the relative abundance of legumin, convicilin, and vicilin, compared to controls, with the O_3 and OH treatments having the greatest effect (Fig. 3**b**, Table 1). ROS, especially OH radicals as well as O_3, preferably attack sulfur-containing amino acids (Segat et al., 2014; Surowsky, Bußler, & Schlüter, 2016), resulting in the formation of inter- and intra-chain disulfide linkages. While the relative abundance of soluble aggregates in pH 2 PPI control was higher than that of pH 7 PPI control, it was not as high as in the mPPI samples, indicating that the treatment with plasma species had more pronounced effect on the formation of soluble aggregates than that of treatment pH. Acidic pH compared to neutral pH, however, facilitated more interactions with plasma species that resulted in the formation of a relatively higher abundance of soluble aggregates. Since extreme acidic pH will cause protein unfolding as mentioned previously, a higher surface area of the protein was exposed to plasma reactive species at pH 2 than at pH 7. Additionally, O_3 is prone to degradation at high pH more than at low pH solutions (Gardoni, Vailati, & Canziani, 2012). Therefore, it is reasonable that plasma species had a bigger impact on the protein structure at pH 2 than at pH 7. Because of the higher impact of treatment at pH 2, further characterization was performed on mPPI samples that were treated at pH 2 and dialyzed to remove salt interference.

3.4. Effect of plasma species on the protein denaturation state

Interaction of plasma species with the protein can result in protein unfolding, i.e., denaturation. Several studies have reported protein denaturation/unfolding upon CAP treatment (Ekezie et al., 2019; Sharifian et al., 2019). Therefore, in this study, DSC was performed to determine the impact of different plasma reactive species on the denaturation state of proteins in PPI. Two endothermic peaks corresponding

Table 2
Denaturation temperatures and enthalpy, secondary structure, surface hydrophobicity and surface charge of commercial pea protein reference, non-modified pea protein controls, and plasma modified pea protein isolates at pH 2 (with dialysis).

Samples	Denaturation Temperature and Enthalpy				Surface Properties		Secondary Structure			
	Vicilin		Legumin		Surface Hydrophobicity	Surface Charge	α Helix	β Sheet	β Turn	Random Coil
	Denaturation Temperature (Td, °C)	Enthalpy of Denaturation (ΔH, J g-1)	Denaturation Temperature (Td, °C)	Enthalpy of Denaturation (ΔH, J g-1)	RFI	mV	Relative Percentage			
cPPI	*1	*	*	*	12719[a]	−27.2[a]	14.5[b]	46.3[bc]	24.8[a]	14.5[a]
PPI Control-pH7	84.5[2a]	6.39[a]	91.4	1.48	8545[d]	−37.6[b]	23.3[a]	44.9[c]	22.8[b]	9.02[a]
PPI Control-pH2	81.7[b]	2.45[b]	*	*	9148 [cd]	−37.8[b]	22.7[a]	46.0[bc]	18.8[bc]	12.5[a]
mPPI-N_xO_y/O_3 pH2	80.2[c]	1.84[c]	*	*	10393[bcd]	−39.5[b]	23.0[a]	42.8[c]	20.6[bc]	13.5[a]
mPPI- O_3 pH2	80.7[bc]	1.28[d]	*	*	11964[ab]	−38.8[b]	20.2[a]	51.3[a]	19.4[bc]	9.15[a]
mPPI-H_2O_2 pH2	82.1[b]	1.98[c]	*	*	11095[abc]	−38.6[b]	21.0[a]	50.1[ab]	19.0[bc]	10.0[a]
mPPI- OH pH2	81.5[bc]	1.13[d]	*	*	12386[ab]	−38.5[b]	19.3[ab]	53.3[a]	13.3[c]	14.2[a]

[1]An asterisk (*) represents no peak of denaturation observed;
[2]Means (n = 3) in each column with different lowercase letters indicate significant differences among samples, according to the Tukey-Kramer multiple means comparison test ($P < 0.05$).

to vicilin and legumin were observed in pH 7 PPI control (Table 2). Convicilin did not show up as a separate endothermic peak on the thermogram. This observation can be primarily attributed to the structural similarity between convicilin and vicilin, and thus potentially showing up as one endothermic peak. As, expected, no endothermic peaks were observed for cPPI reference, indicating complete denaturation. cPPI might have been subjected to severe extraction and processing conditions that lead to denaturation and the subsequent polymerization discussed earlier (Fig. 2**b**). On the other hand, pH 2 control had only one endothermic peak for vicilin, with significantly lower enthalpy compared to the pH 7 control. The extreme acidic pH resulted in protein unfolding as noted by the complete disappearance of the legumin endothermic peak, and the marked reduction in the denaturation enthalpy of vicilin. It is worth noting that legumin abundance in pea protein is much lower than that of vicilin (vicilin: legumin up to 8:1) (Tzitzikas et al., 2006), hence its endothermic peak could be hard to detect or distinguish from the adjacent vicilin peak, especially when significant unfolding occurs. Reactive species treatment at pH 7 had hardly any impact on the protein denaturation state (Table S3). The significantly higher denaturation temperature for vicilin, observed for non-dialyzed mPPIs treated at pH 2, was attributed to the presence of high amount of salt (Table S3). In dialyzed samples, the denaturation temperature of vicilin in mPPIs treated at pH 2 was similar to that of the control sample. Compared to pH 2 control, treatment with plasma species resulted in further significant reduction in the denaturation enthalpy of vicilin, with O_3 and OH radicals having the most impact (Table 2). As aforementioned, O_3 (Segat et al., 2014) and OH radicals (Surowsky et al., 2016) are impactful plasma reactive species that oxidize sulfide-containing amino acids. The unfolding process is a result of the disruption of non-covalent interactions within the protein, triggered by the energy input of CAP. The unfolding process of the protein could be then facilitated during the formation of inter-chain disulfide interchange. Moreover, the proximity of two proteins caused by newly formed disulfide linkages could lead to further unfolding of the proteins due to steric hindrance from adjacent side chains. This observation further explains the higher abundance of soluble aggregates in PPI samples treated with O_3 and OH radicals (Fig. 3, Table 1), since unfolded proteins have higher tendency to polymerize.

3.5. Effect of plasma species on the protein surface properties

The unfolding of the globular protein leads to the exposure of the hydrophobic core, thus increasing surface hydrophobicity. Increases in surface hydrophobicity impact protein interactions and thus functional properties such as solubility, gelation, and emulsification. Segat et al. (2015) reported a significant increase in surface hydrophobicity of whey protein, and improved emulsifying and foaming properties after DBD (air) treatment that was comprised of a mixture of N_xO_y and O_3. Similar observation in surface hydrophobicity was also reported by Ekezie et al. (2019). However, the impact of various reactive species on the unfolding process was not clear. Therefore, changes in surface hydrophobicity were monitored as impacted by plasma species treatment (Table 2) in comparison to the reference sample, cPPI, and the PPI controls. The reference cPPI exhibited the highest surface hydrophobicity among all samples, complementing denaturation data and degree of polymerization discussed earlier. Plasma species treatment at pH 7 had no significant impact on surface hydrophobicity (Table S3). However, a significant increase in surface hydrophobicity was observed after treatment with O_3 and OH at pH 2 compared to pH 2 and pH 7 controls (Table 2). These results complemented the observed impact of O_3 and OH reactive species at pH 2 on denaturation and unfolding. Increases in surface hydrophobicity were observed after treatment with N_xO_y/O_3 at pH 2 but were not statistically significant. Although a similar amount of O_3 was produced in both N_xO_y/O_3 and O_3 treatments, the presence of RNS appeared to reduce the O_3 effect on protein unfolding. Lukes, Dolezalova, Sisrova, and Clupek (2014) found that the presence of RNS such as nitrites were able to rapidly decompose O_3 in liquid and generate oxygen molecules instead. Therefore, compared to O_3 treatment, RNS/O_3 treatment had less impact on the denaturation state of the proteins in PPI.

Another important protein surface property is the surface charge (zeta potential, ζ), which, together with surface hydrophobicity, has a direct bearing on the protein's solubility, gelation and emulsification properties. Protein denaturation and polymerization could also affect the surface charge due to changes in conformation and relative exposure of different groups. Accordingly, the surface charge as impacted by plasma species treatment was monitored.

The surface charge of the pH 7 PPI control was -37.6 mV, similar to previously reported values (Ladjal-Ettoumi, Boudries, Chibane, & Romero, 2016). The net surface charge of cPPI was significantly lower than that of the PPI controls, an observation attributed to its high degree of denaturation and polymerization induced by extreme processing conditions, resulting in the formation of insoluble aggregates. In non-dialyzed pH 2 samples, the high salt content contributed to a significant decrease in surface charge (Table S3). However, the surface charge was restored upon dialysis, revealing no significant impact of plasma species treatment (Table 2). This could be attributed to the formation of high molecular weight soluble aggregates, which could be highly charged due to moderate unfolding and polymerization of proteins induced by plasma treatment. Maintenance of high surface charge will have a positive impact on functionality. Mahdavian Mehr and Koocheki (2020), on the other hand, reported a significant increase in the surface net charge of pea protein after DBD (air) treatment. They attributed this observation to the oxidation of certain amino acids that could have led to the formation of negatively charged amino acids. Reports on changes in zeta potential after CAP treatment are limited.

3.6. Effect of plasma species on the protein secondary structure

In addition to protein profile, protein denaturation state, and surface properties, protein secondary structure was also impacted by the reactive species. The relative abundance of α helix, β sheet, β turn and random coil in pH 7 PPI control (Table 2) was similar to that reported by Beck, Knoerzer, and Arcot (2017). The reference cPPI had the least relative amount of α helix, and the lowest ratio of α helix to β sheet, indicating protein denaturation at the secondary structure level (Ekezie et al., 2019). As with other structural data presented thus far, treatment at pH 7 had no significant impact on the protein secondary structure (Table S3). On the other hand, the relative abundance of the β-sheet in PPI samples treated with O_3 or OH radicals was significantly higher than that of PPI controls. Accordingly, the α-helix to β-sheet ratio in PPI was significantly reduced after O_3 and OH treatment, which also indicated denaturation at the secondary structure level. Protein polymerization and unfolding induced by O_3 and OH radicals could be responsible for the increases in β-sheet content. The formation of interchain β-sheet could be initiated by proximity of proteins and exposed amino acids residues, caused by polymerization and unfolding, respectively. Several studies also reported similar secondary structure changes after CAP treatment (Ekezie et al., 2019; Ji et al., 2018; Sharifian et al., 2019). Sharifian et al. (2019) observed a decrease in α helix content, while Ji et al. (2018) reported an increase in β sheet content and a decrease in α helix content, after air DBD treatment. The increase in β sheet content after CAP treatment could directly improve protein functionality. For example, amyloid fibrils produced from plant protein isolates, which were only comprised of β sheet structure, exhibited significantly improved emulsification and gelling properties compared to original counterparts (Cao & Mezzenga, 2019).

3.7. Effect of plasma species on protein functionality

Protein solubility is an important functionality as it can influence several other functional properties, including gelation and

emulsification. Adequate protein solubility is needed for utilization in food systems, especially in high protein beverage applications. Contradictory solubility results after CAP treatment were observed in different studies. Contradictory findings are attributed to differences in the conditions of the reported solubility tests, as well as differences in the intensity and profile of the plasma reactive species. Ekezie et al. (2019) reported a decrease in protein solubility after atmospheric pressure plasma jet (APPJ) treatment in air, whereas Bußler et al. (2015) reported an increase in protein solubility after air DBD treatment. Ekezie et al. (2019) observed a decrease in pH during APPJ treatment, but APPJ-treated samples were directly tested for solubility without adjusting the pH to resemble that of the control. The pH after the APPJ treatment was close to the isoelectric point of the protein, thus explaining the reduced solubility. Bußler et al. (2015), on the other hand, compared the solubility of DBD treated samples to that of the control at the same pH. Moreover, different plasma units and power sources were used in the two studies, thus contributing to differences in intensities and profiles of the generated plasma reactive species, which could further explain the contradictory solubility results. Accordingly, in this study, the pH of the treated protein solution was adjusted to 7 and lyophilized prior to testing solubility. Thus, any changes in protein solubility were directly attributed to the treatment with the different plasma species.

Given that treatment at pH 7 did not impart major changes in the protein profile and structure, changes in functional properties were minimal (Table S4). On the other hand, significant functionality enhancement, in comparison to the controls as well as the reference cPPI, was noted for PPI samples treated with different plasma species at pH 2 (Table 3).

The reference cPPI exhibited the lowest protein solubility under both heated and non-heated conditions (Table 3). This observation was largely attributed to the high degree of denaturation at both the secondary and tertiary level, high level of polymerization and insoluble aggregates, high surface hydrophobicity, and comparatively low surface charge. The PPI samples treated with O_3 and OH radicals had comparable solubility to that of pH 7 PPI control, and significantly higher solubility under non-heated condition than that of the pH 2 PPI control. The observed increase in solubility could be mostly attributed to the formation of soluble aggregates and the retained high surface charge, which could have offset the observed increase in surface hydrophobicity.

The reference cPPI and the PPI controls did not form a gel at 15% protein concentration (Table 3). This observation confirmed their poor gelling ability. Even at 20% protein concentration, both the reference cPPI and the pH 7 control PPI had low gel strength. The low gelling properties of cPPI could be attributed to its low solubility, high level of denaturation and aggregation, and imbalance of surface hydrophobicity to the surface charge. To form a well-structured gel, a good hydrophilic/lipophilic balance (HLB) on the protein surface is needed to facilitate protein–protein interactions and protein-water interactions. The low gelling properties of the PPI controls could be attributed to higher proportion of low molecular weight proteins to that of soluble aggregates, which promote gel matrix formation. On the other hand, PPI samples treated with O_3, N_xO_y/O_3 mixture, and OH species formed a gel at 15% protein, and had the greatest gel strength at 20% protein concentration. This observation could be attributed to the enhanced protein solubility, increases in soluble aggregates, and the potentially good balance between surface hydrophobicity and surface charge. The gelling properties of pea protein as impacted by CAP treatment has not been reported previously. The results of this study demonstrate the potential of using CAP that enable the delivery of O_3 and OH species, to improve the gelling properties of pea protein isolates.

The reference cPPI exhibited the lowest emulsification capacity (EC), again mostly due to high level of denatured, aggregated, and insoluble proteins with low surface charge (Table 3). The EC was significantly increased after treatment with all plasma species, compared to pH 7 control. The EC of pH 2 control PPI was significantly higher than that of the pH 7 control, and was comparable to the samples treated with N_xO_y/O_3 and H_2O_2, indicating in this case that the enhancement was only attributed to the structural changes induced by the acidic environment. In contrast, treatments with O_3 and OH radicals resulted in further enhancement in EC, an observation attributed to the significantly different structural characteristics. Good HLB and flexible protein structures are required to interact with both oil and water phases. Accordingly, the enhanced EC after treatment with O_3 and OH could be attributed to good solubility, favorable balance between surface charge and hydrophobicity, increased β-sheet content, partially unfolded and thus more flexible proteins, and the relatively high amounts of soluble aggregates that could form a strong protein film at the interface. Segat et al. (2015), Ji et al. (2018), and Mahdavian Mehr and Koocheki (2020) reported an enhancement in emulsification properties of whey, peanut, and pea protein, respectively, after air DBD treatment. Since DBD treatment used in these studies was remote with negligible water content in the dry compressed air, the impact of any plasma-generated OH radicals can be neglected, thus the enhanced emulsification properties were largely attributed to O_3. Since the presence of N_xO_y appeared to reduce the O_3 effect on the structure and functionality of PPI, O_2 instead of air seemed to have advantages as feed gas to generate plasma that could significantly enhance functionality. Additionally, due to the significant effect of OH radicals, generated in this study from the Fenton's reaction, on the structure of the proteins, direct plasma application to the protein solution, allowing the production of OH radicals, might be beneficial to further enhance functional properties.

4. Conclusions

For the first time, the findings of this work successfully demonstrated the impact of different plasma-produced reactive species (N_xO_y/O_3, O_3, H_2O_2, and OH) on the secondary, tertiary, and quaternary structures of pea protein, and the consequent changes in functional properties. Results can be used to explain previously reported observations related to

Table 3
Solubility, gel strength and emulsification capacity of commercial pea protein reference, non-modified pea protein controls, and plasma modified pea protein isolates at pH 2 (with dialysis).

Samples	Solubility (5% protein)		Gel Strength (15% protein)	Gel Strength (20% protein)	Emulsification Capacity (2% protein)
	Non-Heated	Heated (80 °C for 30 min)	Strength (N)	Strength (N)	mL oil/g protein
cPPI	23.9[2c]	41.9[b]	*[1]	2.73[d]	229.4[d]
PPI Control- pH7	82.4[a]	79.6[a]	*	5.69 [cd]	341.0[c]
PPI Control- pH2	66.9[b]	76.0[a]	*	11.7[bc]	644.8[b]
mPPI- N_xO_y /O_3 pH2	78.1[a]	81.9[a]	2.21[a]	21.9[a]	685.1[b]
mPPI- O_3 pH2	81.6[a]	83.7[a]	3.34[a]	25.2[a]	809.1[a]
mPPI- H_2O_2 pH2	71.2[b]	75.5[a]	*	12.1[bc]	634.0[b]
mPPI- OH pH2	80.0[a]	84.3[a]	1.23[a]	18.5[ab]	823.1[a]

[1]An asterisk (*) represents no measurable gels formed at 15% protein concentration;
[2]Means (n = 3) in each column with different lowercase letters indicate significant differences among samples, according to the Tukey-Kramer multiple means comparison test ($P < 0.05$).

the impact of different CAP systems on the functional properties of proteins. These results can also be used to optimize CAP treatment, in terms of plasma species production, to induce specific structural changes and a directed enhancement in functionality. Results indicated that O_3 and OH radicals are the most impactful species on the pea protein structure among all four investigated species. In addition, results highlighted that plasma sources that could effectively generate O_3 and OH radicals (oxidizing species) are preferable for pea protein functionalization. Further investigation on the role of N_xO_y on protein modification is needed to further optimize CAP treatments. Finally, characterization of the interaction of O_3 and OH radicals with specific amino acid residues could further explain the observed structural changes. Nevertheless, this work provides a detailed understanding of the potential of CAP and associated reactive species in enhancing pea protein functionality.

CRediT authorship contribution statement

Fan Bu: Conceptualization, Methodology, Investigation, Formal analysis, Writing - original draft. **Gaurav Nayak:** Methodology, Writing - review & editing. **Peter Bruggeman:** Conceptualization, Methodology, Writing - review & editing. **George Annor:** Conceptualization, Writing - review & editing. **Baraem P Ismail:** Conceptualization, Project administration, Writing - review & editing, Funding acquisition.

Declaration of Competing Interest

The authors declare that they have no known competing financial interests or personal relationships that could have appeared to influence the work reported in this paper.

Acknowledgments

This project was generously funded by the Plant Protein Innovation Center (PPIC). FTIR-ATR data collection of this work was carried out in the Characterization Facility, University of Minnesota, which receives partial support from the NSF through the MRSEC (Award Number DMR-2011401) and the NNCI (Award Number ECCS-2025124) programs.

Appendix A. Supplementary data

Supplementary data to this article can be found online at https://doi.org/10.1016/j.foodchem.2021.131135.

References

Arteaga, V. G., Guardia, M. A., Muranyi, I., Eisner, P., & Schweiggert-Weisz, U. (2020). Effect of enzymatic hydrolysis on molecular weight distribution, techno-functional properties and sensory perception of pea protein isolates. *Innovative Food Science & Emerging Technologies, 65*, Article 102449.

Bahrami, N., Bayliss, D., Chope, G., Penson, S., Perehinec, T., & Fisk, I. D. (2016). Cold plasma: A new technology to modify wheat flour functionality. *Food Chemistry, 202*, 247–253.

Barać, M., Čabrilo, S., Pešić, M., Stanojević, S., Pavlićević, M., Maćej, O., & Ristić, N. (2011). Functional Properties of Pea (Pisum sativum, L.) Protein Isolates Modified with Chymosin. *International Journal of Molecular Sciences, 12*(12), 8372–8387. https://doi.org/10.3390/ijms12128372.

Barac, M., Cabrilo, S., Pesic, M., Stanojevic, S., Zilic, S., Macej, O., & Ristic, N. (2010). Profile and functional properties of seed proteins from six pea (Pisum sativum) genotypes. *International Journal of Molecular Sciences, 11*(12), 4973–4990. https://doi.org/10.3390/ijms11124973.

Barac, M., Cabrilo, S., Stanojevic, S., Pesic, M., Pavlicevic, M., Zlatkovic, B., & Jankovic, M. (2012). Functional properties of protein hydrolysates from pea (Pisum sativum, L) seeds. *International Journal of Food Science & Technology, 47*(7), 1457–1467.

Beck, S. M., Knoerzer, K., & Arcot, J. (2017). Effect of low moisture extrusion on a pea protein isolate's expansion, solubility, molecular weight distribution and secondary structure as determined by Fourier Transform Infrared Spectroscopy (FTIR). *Journal of Food Engineering, 214*, 166–174. https://doi.org/10.1016/j.jfoodeng.2017.06.037.

Björck, I., & Asp, N.-G. (1983). The effects of extrusion cooking on nutritional value—A literature review. *Journal of Food Engineering, 2*(4), 281–308.

Boekema, B., Vlig, M., Guijt, D., Hijnen, K., Hofmann, S., Smits, P., … Middelkoop, E. (2015). A new flexible DBD device for treating infected wounds: In vitro and ex vivo evaluation and comparison with a RF argon plasma jet. *Journal of Physics D: Applied Physics, 49*(4), Article 044001.

Boyle, C., Hansen, L., Hinnenkamp, C., & Ismail, B. P. (2018). Emerging camelina protein: Extraction, modification, and structural/functional characterization. *Journal of the American Oil Chemists' Society, 95*(8), 1049–1062.

Brückner-Gühmann, M., Heiden-Hecht, T., Sözer, N., & Drusch, S. (2018). Foaming characteristics of oat protein and modification by partial hydrolysis. *European Food Research and Technology, 244*(12), 2095–2106.

Bruggeman, P., & Schram, D. C. (2010). On OH production in water containing atmospheric pressure plasmas. *Plasma Sources Scinece and Technology, 19*(4), 045025. https://doi.org/10.1088/0963-0252/19/4/045025.

Bußler, S., Steins, V., Ehlbeck, J., & Schlüter, O. (2015). Impact of thermal treatment versus cold atmospheric plasma processing on the techno-functional protein properties from Pisum sativum 'Salamanca'. *Journal of Food Engineering, 167*, 166–174.

Cao, Y., & Mezzenga, R. (2019). Food protein amyloid fibrils: Origin, structure, formation, characterization, applications and health implications. *Advances in Colloid and Interface Science, 269*, 334–356.

Chao, D., & Aluko, R. E. (2018). Modification of the structural, emulsifying, and foaming properties of an isolated pea protein by thermal pretreatment. *CyTA-Journal of Food, 16*(1), 357–366.

Chao, D., Jung, S., & Aluko, R. E. (2018). Physicochemical and functional properties of high pressure-treated isolated pea protein. *Innovative Food Science & Emerging Technologies, 45*, 179–185.

Ekezie, F.-G., Cheng, J.-H., & Sun, D.-W. (2019). Effects of atmospheric pressure plasma jet on the conformation and physicochemical properties of myofibrillar proteins from king prawn (Litopenaeus vannamei). *Food Chemistry, 276*, 147–156.

Farr, J. P., Smith, W. L., & Steichen, D. S. (2000). Bleaching agents. *Kirk-Othmer Encyclopedia of Chemical Technology*.

Gardoni, D., Vailati, A., & Canziani, R. (2012). Decay of ozone in water: A review. *Ozone: Science & Engineering, 34*(4), 233–242.

Gatehouse, J. A., Lycett, G. W., Croy, R. R. D., & Boulter, D. (1982). The post-translational proteolysis of the subunits of vicilin from pea (Pisum sativum L.). *Biochemical Journal, 207*(3), 629–632. https://doi.org/10.1042/bj2070629.

Ge, J., Sun, C. X., Corke, H., Gul, K., Gan, R. Y., & Fang, Y. (2020). The health benefits, functional properties, modifications, and applications of pea (Pisum sativum L.) protein: Current status, challenges, and perspectives. *Comprehensive Reviews in Food Science and Food Safety, 19*(4), 1835–1876.

Gorbanev, Y., Privat-Maldonado, A., & Bogaerts, A. (2018). Analysis of short-lived reactive species in plasma–air–water systems: The dos and the do nots. *Analytical Chemistry, 90*(22), 13151–13158. https://doi.org/10.1021/acs.analchem.8b03336.

Harris, J., Phan, A. N., & Zhang, K. (2018). Cold plasma catalysis as a novel approach for valorisation of untreated waste glycerol. *Green Chemistry, 20*(11), 2578–2587.

Ismail, B. P., Senaratne-Lenagala, L., Stube, A., & Brackenridge, A. (2020). Protein demand: Review of plant and animal proteins used in alternative protein product development and production. *Animal Frontiers, 10*(4), 53–63. https://doi.org/10.1093/af/vfaa040.

Ji, H., Dong, S., Han, F., Li, Y., Chen, G., Li, L., & Chen, Y.e. (2018). Effects of dielectric barrier discharge (DBD) cold plasma treatment on physicochemical and functional properties of peanut protein. *Food and Bioprocess Technology, 11*(2), 344–354.

Kaewruang, P., Benjakul, S., Prodpran, T., Encarnacion, A. B., & Nalinanon, S. (2014). Impact of divalent salts and bovine gelatin on gel properties of phosphorylated gelatin from the skin of unicorn leatherjacket. *LWT-Food Science and Technology, 55*(2), 477–482.

Kutzli, I., Griener, D., Gibis, M., Schmid, C., Dawid, C., Baier, S. K., … Weiss, J. (2020). Influence of Maillard reaction conditions on the formation and solubility of pea protein isolate-maltodextrin conjugates in electrospun fibers. *Food Hydrocolloids, 101*, 105535. https://doi.org/10.1016/j.foodhyd.2019.105535.

Ladjal-Ettoumi, Y., Boudries, H., Chibane, M., & Romero, A. (2016). Pea, chickpea and lentil protein isolates: Physicochemical characterization and emulsifying properties. *Food Biophysics, 11*(1), 43–51.

Lin, D., Zhang, Q., Xiao, L., Huang, Y., Yang, Z., Wu, Z., … Wu, D. (2020). Effects of ultrasound on functional properties, structure and glycation properties of proteins: A review. *Critical Reviews in Food Science and Nutrition*, 1–11.

Lukes, P., Dolezalova, E., Sisrova, I., & Clupek, M. (2014). Aqueous-phase chemistry and bactericidal effects from an air discharge plasma in contact with water: Evidence for the formation of peroxynitrite through a pseudo-second-order post-discharge reaction of H2O2 and HNO2. *Plasma Sources Science and Technology, 23*(1), 015019. https://doi.org/10.1088/0963-0252/23/1/015019.

Mahdavian Mehr, H., & Koocheki, A. (2020). Effect of atmospheric cold plasma on structure, interfacial and emulsifying properties of Grass pea (Lathyrus sativus L.) protein isolate. Food Hydrocolloids, 106, 105899. doi:10.1016/j.foodhyd.2020.105899.

Market Research Future. (2021). Global Plant Protein Ingredients Market Research Report. Retrieved from https://www.marketresearchfuture.com/reports/plant-protein-ingredients-market-5114. Accessed Feburary 2021.

Mirmoghtadaie, L., Shojaee Aliabadi, S., & Hosseini, S. M. (2016). Recent approaches in physical modification of protein functionality. *Food Chemistry, 199*, 619–627. https://doi.org/10.1016/j.foodchem.2015.12.067.

Moldgy, A., Nayak, G., Aboubakr, H. A., Goyal, S. M., & Bruggeman, P. J. (2020). Inactivation of virus and bacteria using cold atmospheric pressure air plasmas and the role of reactive nitrogen species. *Journal of Physics D: Applied Physics, 53*(43), 434004. https://doi.org/10.1088/1361-6463/aba066.

Nayak, G., Aboubakr, H. A., Goyal, S. M., & Bruggeman, P. J. (2018). Reactive species responsible for the inactivation of feline calicivirus by a two-dimensional array of

integrated coaxial microhollow dielectric barrier discharges in air. *Plasma Processes and Polymers, 15*(1), 1700119.

Nayak, G., Du, Y., Brandenburg, R., & Bruggeman, P. J. (2017). Effect of air flow on the micro-discharge dynamics in an array of integrated coaxial microhollow dielectric barrier discharges. *Plasma Sources Science And Technology, 26*(3), 035001. https://doi.org/10.1088/1361-6595/aa56a4.

Nayak, G., Sousa, J. S., & Bruggeman, P. J. (2017). Singlet delta oxygen production in a 2D micro-discharge array in air: Effect of gas residence time and discharge power. *Journal of Physics D: Applied Physics, 50*(10), Article 105205.

Nyaisaba, B. M., Miao, W., Hatab, S., Siloam, A., Chen, M., & Deng, S. (2019). Effects of cold atmospheric plasma on squid proteases and gel properties of protein concentrate from squid (Argentinus ilex) mantle. *Food Chemistry, 291*, 68–76.

Osen, R., Toelstede, S., Wild, F., Eisner, P., & Schweiggert-Weisz, U. (2014). High moisture extrusion cooking of pea protein isolates: Raw material characteristics, extruder responses, and texture properties. *Journal of Food Engineering, 127*, 67–74.

Pankaj, S. K., Misra, N. N., & Cullen, P. J. (2013). Kinetics of tomato peroxidase inactivation by atmospheric pressure cold plasma based on dielectric barrier discharge. *Innovative Food Science & Emerging Technologies, 19*, 153–157.

Pignatello, J. J., Oliveros, E., & MacKay, A. (2006). Advanced oxidation processes for organic contaminant destruction based on the Fenton reaction and related chemistry. *Critical Reviews in Environmental Science and Technology, 36*(1), 1–84.

Prakash, R., Hossain, A. M., Pal, U., Kumar, N., Khairnar, K., & Mohan, M. K. (2017). Dielectric barrier discharge based mercury-free plasma UV-lamp for efficient water disinfection. *Scientific Reports, 7*(1), 1–8.

Segat, A., Misra, N. N., Cullen, P. J., & Innocente, N. (2015). Atmospheric pressure cold plasma (ACP) treatment of whey protein isolate model solution. *Innovative Food Science & Emerging Technologies, 29*, 247–254.

Segat, A., Misra, N. N., Fabbro, A., Buchini, F., Lippe, G., Cullen, P. J., & Innocente, N. (2014). Effects of ozone processing on chemical, structural and functional properties of whey protein isolate. *Food Research International, 66*, 365–372.

Sharifian, A., Soltanizadeh, N., & Abbaszadeh, R. (2019). Effects of dielectric barrier discharge plasma on the physicochemical and functional properties of myofibrillar proteins. *Innovative Food Science & Emerging Technologies, 54*, 1–8.

Surowsky, B., Bußler, S., & Schlüter, O. (2016). Cold plasma interactions with food constituents in liquid and solid food matrices. In *Cold plasma in food and agriculture* (pp. 179–203). Elsevier.

Tolouie, H., Mohammadifar, M. A., Ghomi, H., & Hashemi, M. (2018). Cold atmospheric plasma manipulation of proteins in food systems. *Critical Reviews in Food Science and Nutrition, 58*(15), 2583–2597. https://www.tandfonline.com/doi/pdf/10.1080/10408398.2017.1335689?needAccess=true.

Tzitzikas, E. N., Vincken, J.-P., De Groot, J., Gruppen, H., & Visser, R. G. F. (2006). Genetic Variation in Pea Seed Globulin Composition. *Journal of Agricultural and Food Chemistry, 54*(2), 425–433. https://doi.org/10.1021/jf0519008.